Analytical Methods

ROYAL SOCIETY OF CHEMISTRY

PAPER

View Article Online
View Journal | View Issue

Check for updates

Cite this: *Anal. Methods*, 2023, **15**, 27

Molecularly imprinted polymers as effective capturing receptors in a pseudo-ELISA immunoassay for procalcitonin detection in veterinary species†

Federica Battaglia, *[ab] Francesca Bonelli,[b] Micaela Sgorbini,[b] Luigi Intorre,[b] Maria Minunni,[a] Simona Scarano[a] and Valentina Meucci*[b]

In this study, a new sandwich-type immunoenzymatic assay, based on a molecularly imprinted polymer (MIP) as an artificial antibody (pseudo-ELISA), was developed for the determination of procalcitonin (PCT) in veterinary species. The quantification of PCT in human medicine represents the state of the art for the diagnosis of sepsis; instead the clinical studies on the relevance of PCT as a sepsis predictor in veterinary patients are few, likely due to the total absence of validated assays. MIPs have been widely used as antibody mimics for important applications, and MIP-based sandwich assays have emerged as promising analytical tools for the detection of disease biomarkers. Herein, a polynorepinephrine (PNE)-based imprinted film was directly synthesized on the well surface of a 96-well plate. Subsequently, based on a commercial ELISA kit, the PCT quantification was accomplished *via* a colorimetric sandwich assay by replacing the capture antibody of the kit with the PNE-based MIP. This method was performed to detect canine and equine PCT in buffer and in plasma samples. Under optimal conditions, the results obtained in plasma samples showed a limit of detection (LOD) of 5.87 ng mL^{-1} and a reproducibility ($CV_{av\%}$) of 10.0% for canine samples, while a LOD = 4.46 ng mL^{-1} and $CV_{av\%}$ = 7.61% were obtained for equine samples.

Received 21st July 2022
Accepted 28th November 2022

DOI: 10.1039/d2ay01175a

rsc.li/methods

Open Access Article. Published on 29 november 2022. Downloaded on 19-9-2025 23:44:33.
This article is licensed under a Creative Commons Attribution-NonCommercial 3.0 Unported Licence.

Introduction

Immunoassays, conventionally based on the antibody–antigen reaction, are an essential tool widely used in a multitude of bioanalytical fields for the determination of biomarkers for clinical purposes, food safety, environmental monitoring, and forensic analysis.[1–4] Among the immunoassays, the so-called enzyme-linked immunosorbent assay (ELISA) is considered the gold standard and it is probably the most commonly used method in clinical routine measurement.[5,6] ELISA tests offer significant advantages such as sensitivity and selectivity for the target analyte, are generally convenient for a large sample, and allow the detection of substances from different types of matrices, without pre-treatment and without the need for skilled technicians.[7,8] Capturing receptors of conventional ELISA tests are antibodies, and at present still almost the only choice in the field due to their extraordinary ability in expressing specific sites for molecular recognition against a huge variety of target antigens.[9,10] However, they have many drawbacks correlated to the high cost and the production, together with the need to use laboratory animals. Furthermore antibodies, as proteins, tend to be sensitive to environmental conditions and are physically, chemically and biochemically unstable.

On this basis, molecularly imprinted polymers (MIPs) are excellent versatile tools in different research fields, including biosensing, and have already displayed good performance as an alternative to antibodies capable of binding their target analyte in a specific and selective manner.[11–16] Due to the capability of MIPs to create selective recognition sites in synthetic polymers, they offer the specificity and selectivity of naturally occurring receptors with the explicit improvements of ease and speed of preparation, low cost, and good stability to environmental conditions.[17–20] MIPs have been applied to a wide range of target analytes from small molecules (*e.g.* pesticides, drugs, sugars) to macromolecules such as peptides and proteins.[21–28] At present, there is an increasing interest in the use of these mimetic receptors for the development of diagnostic antibody-free assay employing a variety of sensitive detection methods such as enzymatic amplification (BELISA); radiodetection; fluorescence and chemiluminescence.[29–35] As concerns macromolecule imprinting, the relentless research for new materials for MIP production led to green bio-inspired polymers and in this

[a]*Department of Chemistry "Ugo Schiff", University of Florence, 50019 Sesto Fiorentino, FI, Italy. E-mail: federica.battaglia@unifi.it*

[b]*Department of Veterinary Science, University of Pisa, 56122 Via Livornese, PI, Italy. E-mail: valentina.meucci@unipi.it*

† Electronic supplementary information (ESI) available. See DOI: https://doi.org/10.1039/d2ay01175a

Open Access Article. Published on 29 november 2022. Downloaded on 19-9-2025 23:44:33.
This article is licensed under a Creative Commons Attribution-NonCommercial 3.0 Unported Licence.

perspective, the natural neurotransmitter dopamine (DA) and, more recently, norepinephrine (NE), have played a key role. The two catecholamines share the same ability to easily self-polymerize, under alkaline conditions, to form strongly adherent nanofilms on almost any surface such as noble metals, metal oxides, glass, and synthetic polymers.[35–41] Thanks to these advantageous features, polydopamine (PDA) has already been applied for the development of MIPs both for small molecules[15,31,42–44] and for protein detection.[14,45–51] Compared to its PDA analogue, PNE (polynorepinephrine) exhibits a smoother and more hydrophilic surface, due to the presence of intermediate 3,4-dihydroxybenzaldehyde norepinephrine, that reduces the non-specific adsorption, being particularly advantageous for applications in medical and analytical and bioanalytical fields.[40,52,53] Based on these considerations we have recently developed two biosensors which utilize PDA- and PNE-based MIPs as capturing receptors for equine and canine procalcitonin (PCT) detection in buffer and plasma. In detail, DA and NE were used as monomers for the synthesis of MIP nanofilms directly on surface plasmon resonance (SPR) gold chips and the imprinting efficiencies of proteins were compared.[54] PCT, a prohormone of calcitonin, is encoded by the CALC-1 gene and is synthesized by the C-cells of the thyroid gland. Under normal conditions, PCT is quickly cleaved into three epitopes: (1) an N-terminal region; (2) calcitonin; and (3) katacalcin; therefore, healthy humans commonly have very low levels of plasma PCT ($<0.5\ \mu g\ L^{-1}$).[55,56] In contrast, in systemic microbial infection, the level of the protein increases up to several thousand-fold, within 6 to 12 hours, and in a correlation manner to the severity of infection. Nowadays, the quantification of PCT in human medicine represents the state of the art for the diagnosis of sepsis, the monitoring of disease and antimicrobial stewardship.[57,58] In contrast to the high interest in human procalcitonin, there is no clinical use of PCT in veterinary species and there are very few papers dedicated to its detection.[59,60] Among domestic animals, procalcitonin studies are more in horses than in other species. An increase in the circulating level of PCT has been observed in adult horses during pathological conditions caused by bacteria or by the translocation of bacteria and/or their products into the bloodstream.[61–64] Moreover, under physiological conditions, PCT levels were traced to be higher in horses than in humans due to the different compositions of intestinal bacterial flora.[65] Only about five papers evaluated the plasma levels of canine PCT, showing that septic dogs have higher PCT concentrations than non-septic dogs.[66–69] Regarding cattle, high PCT concentrations were observed in neonatal calves with septicaemic colibacillosis and other pathologic conditions such as respiratory and inflammatory diseases and in staphylococcal mastitis. Furthermore, a positive correlation was noted between PCT and other pro-inflammatory cytokines (*i.e.*, TNF-α and INF-γ) and amyloid A protein, the main acute phase protein studied in cattle for the diagnosis of infections.[70,71]

It is evident that the published studies in the literature for the measurement of PCT principally referred to the human species and include a plethora of papers dedicated to development of innovative analytical methods such as immunological assay and electrochemical and optical biosensors. In the field of veterinary medicine, the search for innovative and appropriate methods for the quantification of PCT is still, today, an ongoing challenge. Moreover, all the published papers dedicated to PCT detection in animals refer to the use of commercially available ELISA kits that are not fully validated in the target species, are expansive, and are useful only for research purposes.[72] Notably, no analytical parameters are reported in the literature for equine PCT ELISA kits, and the only ones present referred to the use of human anti-PCT antibodies, due to the current lack of specific anti-equine antibodies.[73–75] At the same time, acceptable analytical parameters are reported only for one type of canine PCT ELISA kit.[68,69,76] Based on the lack of fully reliable and practical tests, the aim of this work is to develop an innovative analytical assay, for the detection of PCT in veterinary species, by combining the practicality of commercial ELISA kits with the advantages of MIPs. All commonly commercial assays work in a sandwich format in which the first antibody is immobilized on a microplate that serves to capture the antigen, while the secondary antibody (conjugated to an enzyme) is applied as a last step before quantification. The intensity of the signal is directly related to the concentration of the analyte in the sample and involves the horseradish peroxidase (HRP) enzyme as a signal reporter and tetramethylbenzidine (TMB) as a substrate that develops an optical signal in the visible range. Here, commercial ELISA kits were used by replacing the capture antibody with a PNE-based MIP as a capturing receptor for canine and equine PCT detection both in buffer and plasma. For this aim the MIP for equine/canine PCT has been grown on 96-well microplates, obtaining a very sensitive and selective pseudoELISA immunoassay test in a sandwich format with advantages in terms of cost effectiveness and easy preparation of the synthetic receptor.

Experimental

Materials

±-Norepinephrine hydrochloride (NE ≧ 98.0%), tris(hydroxymethyl)aminomethane hydrochloride (Tris–HCl ≧ 99.0%), acetic acid, L-lysine (≧98.0%), L-cysteine hydrochloride monohydrate (≧98.0%) and tris(hydroxymethyl)aminomethane (Tris-base) were purchased from Sigma-Aldrich (Milan, Italy). Recombinant canine procalcitonin (cPCT) and recombinant equine procalcitonin (ePCT) were purchased from Biovendor (Asheville, North Carolina, USA). Polystyrene (PS) 96-well flat-bottom microplates were obtained from Sarstedt (Nümbrecht, Germany).

Two different commercial ELISA kits were used:

(1) Recombinant Canine Procalcitonin ELISA kit (Biovendor Asheville, North Carolina, NC, USA).

(2) Human Procalcitonin DuoSet® ELISA (R&D Systems, Inc, Minneapolis, USA).

Water used for all the preparations was obtained from a Milli-Q system.

Preparation of reagents and buffer solutions

All ELISA kits used in this study are sandwich immunoassays. Reagents and all the buffer solutions were prepared according

 This journal is © The Royal Society of Chemistry 2023

Open Access Article. Published on 29 november 2022. Downloaded on 19-9-2025 23:44:33.
This article is licensed under a Creative Commons Attribution-NonCommercial 3.0 Unported Licence.

to the manufacturer's instructions. The tests were carried out as reported in the technical data sheet. cPCT was measured with the recombinant canine procalcitonin ELISA kit (Biovendor), while ePCT was measured with the human procalcitonin DuoSet® ELISA kit (R&D Systems). Both the commercial kits included dilution buffers, biotin labelled lyophilized antibody, streptavidin-HRP (S-HRP) solutions, wash buffers, substrate solutions (3,3′,5,5′-tetramethylbenzidine, TMB) and stop solutions (H_2SO_4, 2 N). The biotin labelled antibody anti-canine PCT was reconstituted and diluted 1 : 100 just prior to the assay, whereas, for the ePCT detection, the biotinylated sheep anti-human procalcitonin antibody was reconstituted and diluted to a working concentration of 50.0 ng mL^{-1}.

Preparation of imprinted polymers on microplates

PNE-imprinted nanofilms were directly polymerized on the 96-well plate by dropping a monomer solution (100 μL per well) prepared by mixing NE, at a concentration of 5.00 mg mL^{-1} in 20.0 mmol L^{-1} Tris–HCl (pH 8.50), in the presence of the template (cPCT/ePCT) at four different concentrations (0.500, 5.00, 50.0 and 500 ng mL^{-1}). For simplicity, in the text, the MIP imprinted with cPCT is renamed cMIP, whereas the one imprinted with ePCT is renamed eMIP. The plates were left upside down and the polymerization was conducted at 25.0 °C for 5 hours. After polymerization was complete, the 96-well plates were washed with deionized water to remove unreacted reagents and then a surface passivation step was performed according to the following procedure: 100 μL of an aqueous solution consisting of 1.00 mmol L^{-1} cysteine, 1.00 mmol L^{-1} lysine and 1.00 mmol L^{-1} tris(hydroxymethyl)aminomethane was dropped onto the MIP surface and left overnight at 25.0 °C by avoiding evaporation. The passivation step is based on the Michael addition reaction and allows the covalent binding of the amines and thiols to the PNE surface in order to minimize possible non-specific interactions of biomolecules present in biological matrices. Finally, the plates were washed with acetic acid (aq. 5.00% v/v, 200 μL per well) three times to remove the template from the MIP, and then with deionized water (200 μL per well, three times).

Sandwich assay protocols

Canine PCT. The sandwich assay for quantitative detection of cPCT was carried out using the commercial ELISA kit for recombinant canine procalcitonin (Biovendor) by replacing the capturing Ab with the imprinted film (cMIP), directly grown on the 96-well microplate. Moreover, the Biovendor kit is the only one for which acceptable analytical parameters are reported in the literature.[68,69,72,76] The preparation of reagents and all incubations and washes were performed according to the manufacturer's instructions with slight modifications. Briefly 100 μL of diluent buffer (blank wells) and 100 μL of standard PCT properly diluted in the same buffer at different concentrations (5.00, 10.0, 12.5, 25.0, 50.0 and 100 ng mL^{-1}) were added, in triplicate, into the appropriate wells. The plate was incubated at room temperature (*ca.* 25.0 °C) for 1 hour, by shaking at *ca.* 300 rpm on an orbital microplate shaker. After being washed with the washing buffer three times (350 μL per well), to each well on the plate, 100 μL of biotin labelled solution was added

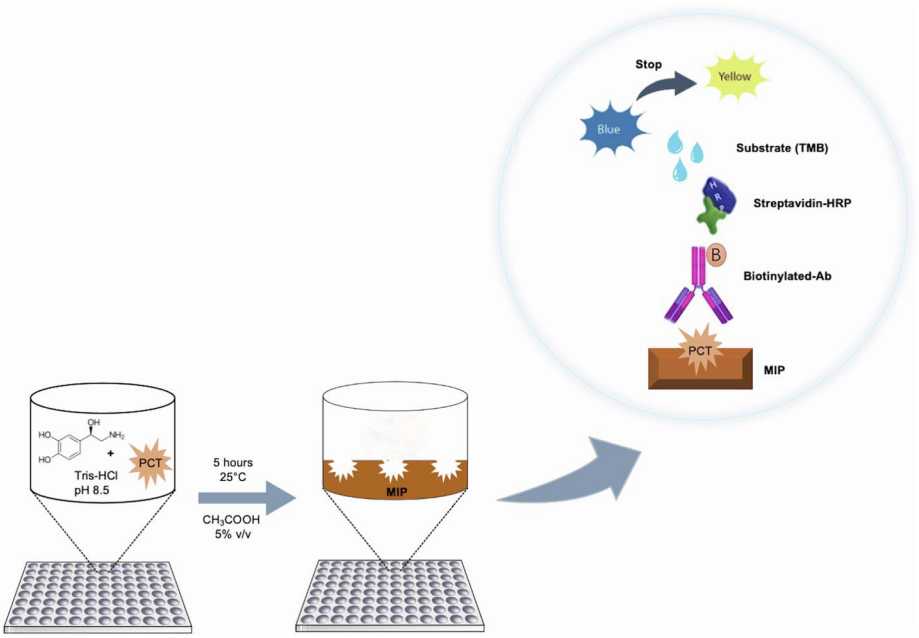

Fig. 1 Schematic illustration of the imprinting process onto the 96-well microplate and the MIP-based ELISA sandwich. The functional monomer (NE) and the template (PCT) were dropped as a mixture on the 96-well plates and the polymerization was conducted at 25 °C for 5 hours. Then, the template was washed out of the polymeric matrix, and the sandwich assay was set up by using a secondary biotinylated antibody following analyte (PCT) addition. After the washing steps, streptavidin conjugated with the enzyme HRP is added to bind the biotinylated antibody; after the final washing, the substrate TMB is added, and color development is observed.

Open Access Article. Published on 29 november 2022. Downloaded on 19-9-2025 23:44:33.
This article is licensed under a Creative Commons Attribution-NonCommercial 3.0 Unported Licence.

and incubated as above. Then, the streptavidin-HRP conjugate (100 μL per well) was added, and the plate was incubated for 30 minutes. After the final wash process, 100 μL of substrate solution was added to each well and the plate was incubated in the dark at room temperature for 15 min without shaking. The reaction was stopped by adding 100 μL of the stop solution (Fig. 1). The absorbance was determined for each well using a microplate reader (Synergy HTX, BioTek, Ahsi S.p.A., Bernareggio, MB, Italia) and by subtracting the readings at 630 nm from the readings at 450 nm.

Equine PCT. Equine PCT was measured with commercial ELISA kits for human PCT (DuoSet® ELISA) by replacing the capturing Ab with the imprinted film (eMIP). According to DuoSet's instructions 100 μL of standard ePCT, properly diluted in buffer at different concentrations (50.0, 100, 200, 400 and 600 ng mL^{-1}), was added into the appropriate well (three replicates), and the plate was incubated at room temperature (*ca.* 25.0 °C) for 2 hours, by shaking at *ca.* 300 rpm on an orbital microplate shaker. After being washed three times (300 μL per well) with the washing buffer, 100 μL of biotin labelled antibody (50.0 ng mL^{-1}) was added and incubated as above. Afterwards, the washing process was repeated and streptavidin-HRP (100 μL per well) was incubated for 20 minutes. Finally, 100 μL of substrate solution was added to each well and the plate was incubated in the dark at room temperature for 20 min. The reaction was stopped by adding 50.0 μL of the stop solution. The absorbance was determined for each well by subtracting the readings at 540 nm from the readings at 450 nm. For both the proteins, the standard curve was constructed by plotting the mean absorbance of the standard against the known concentration for all ELISA kits. The absorbance of the blanks was subtracted from each sample absorbance.

Analysis of procalcitonin in plasma samples

The sandwich assays were further tested to detect PCT in spiked horse and dog plasma samples. Blood samples were collected from healthy animals at the Department of Veterinary Science of the University of Pisa. After collection, samples were immediately centrifuged at 3000 rpm for 10 min and plasma aliquots were stored at −80.0 °C from the time of collection and thawed just before use. Hence, the canine/equine plasma samples were diluted 1 : 10 properly in buffer and spiked respectively, with a known amount of cPCT at concentrations of 25.0, 50.0, 100, 200 and 400 ng mL^{-1} and ePCT at concentrations of 200, 400, 600, 800 and 1000 ng mL^{-1}. Spiked samples were explored following the same experimental procedure reported above (see paragraph 2.1.4).

Results and discussion

Optimization of the experimental conditions

The template concentration (cPCT/ePCT) to be used during PNE imprinting was first optimized to obtain the highest binding performances with the imprinted material. The concentration of the template theoretically reflects the density of binding sites obtained on the MIP surface; therefore, choosing the right concentration is a crucial step of the imprinting process. For both the proteins, the MIPs were synthesized by using four different concentrations of the template (0.500, 5.00, 50.0 and 500 ng mL^{-1}) leaving the starting concentration of the functional monomer (5.00 mg mL^{-1}) unchanged. As shown in Fig. 2a and b, an excellent linearity was obtained for all the tested concentrations for both proteins. In detail, for cPCT (Fig. 2a), a significantly lower absorbance signal was observed at 500 ng mL^{-1}; therefore the highest template concentration was not further considered. Conversely, the best binding ability and the higher absorbance signal were observed for the three lower densities of imprinting (0.500, 5.00 and 50.0 ng mL^{-1}). Among these concentrations, almost overlapping responses were obtained, except for a slight improvement trend that was noted with the decreasing template concentration. For this reason, the

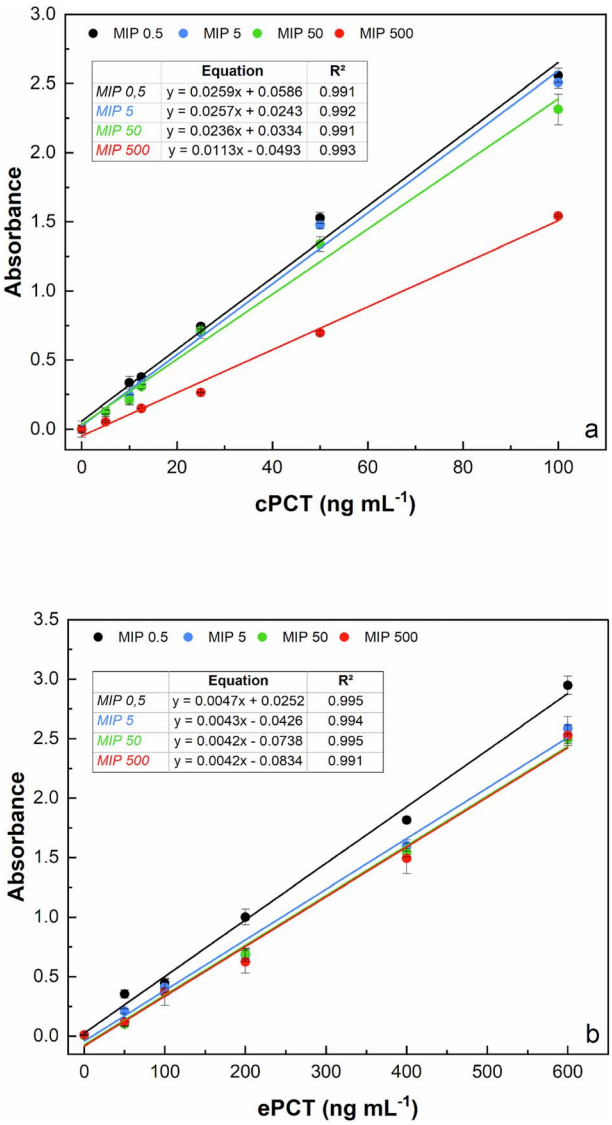

Fig. 2 Comparison of calibration curves obtained in buffer for cPCT (a) and ePCT (b) on MIPs imprinted with four different concentrations (0.500, 5.00, 50.0 and 500 ng mL^{-1}) of the template (cPCT and ePCT respectively).

This journal is © The Royal Society of Chemistry 2023

Open Access Article. Published on 29 november 2022. Downloaded on 19-9-2025 23:44:33.
This article is licensed under a Creative Commons Attribution-NonCommercial 3.0 Unported Licence.

subsequent experiments were conducted by using 0.500 ng mL^{-1} as the template, especially considering that in this study the whole protein was used as a template for MIP synthesis. Instead, for ePCT (Fig. 2b), a different behaviour was observed: similar responses were recorded for template concentrations of 5.00, 50.0 and 500 ng mL^{-1}, whereas an improvement of the absorbance signal was obtained for the lower density of imprinting (0.500 ng mL^{-1}).

It is interesting that the absorbance signal increases, for both biomarkers, in an inverse way to the concentration of the template, while it does not increase the absorbance of the negative control (dilution buffer without PCT). This might be attributed to the fact that during the copolymerization, the lower concentration of the template minimizes the steric crowding of the molecules leading to a more efficient creation of the binding cavities for PCT. On the other hand, higher template concentrations could have excessively reduced the amount of norepinephrine available for polymerization, resulting in the formation of insufficient specific cavities for the recognition of the template molecule. On this basis, subsequent experiments were conducted by using 0.500 ng mL^{-1} as a template concentration for MIP synthesis for canine and equine procalcitonin.

Sandwich assay on MIP-coated microplates

Canine PCT. Once the template concentration for MIP imprinting was optimized, the sandwich assay was performed according to the protocols reported in the Materials and Methods section. Briefly, the PNE-based MIP for cPCT detection was first grown on the surface of a transparent 96-well plate and the sandwich assay was directly carried out. A biotinylated secondary antibody was used for signal amplification; thus, the target antigen was bound between the MIP and the detection antibody. In this case, biotinylated anti-PCT was conjugated to the signal reporter, S-HRP, to develop a colorimetric reaction by using TMB as the substrate. The signal produced was directly dependent on the enzyme–substrate pair used for detection and it was directly proportional to PCT concentrations. The standard curve with cPCT in buffer (Fig. 3a) was constructed within the range of 5.00–100 ng mL^{-1} and showed a correlation coefficient (R^2) of 0.993. The signals measured were expressed as the absorbance of the standard sample minus the absorbance of the blank wells. The values shown in the graph were obtained from the average of five calibration curves based on the analysis of triplicate standard solutions. The limits of detection (LOD) and quantification (LOQ) were calculated as three times and ten times the standard deviation, for the blank sample, divided by the slope of the standard curve, resulting in 3.75 ng mL^{-1} and 12.5 ng mL^{-1}, respectively. Furthermore, the reproducibility of the assay was calculated in terms of intra-assay and inter-assay variability and expressed as an average of coefficient of variation (CV_{av}%). In detail, four replicates for each concentration were considered for the calculation of the intra-assay CV%, while five calibration curves were analyzed for the calculation of the inter-assay CV%. The CV_{av}% resulted in 2.82% and 6.57%, respectively.

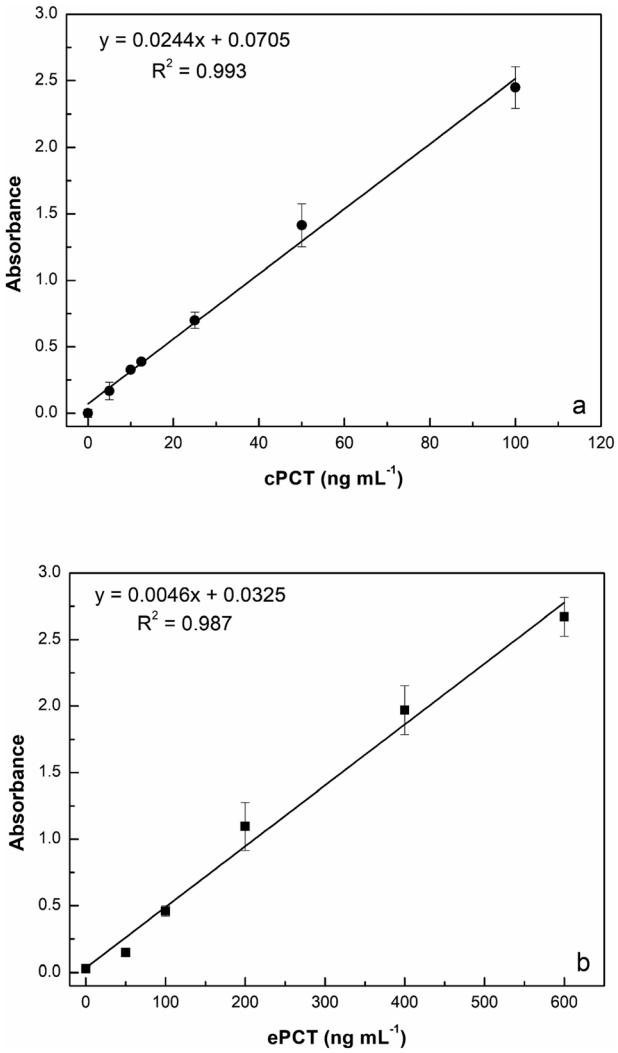

Fig. 3 Linear fitting obtained for cPCT on cMIPs (a) and ePCT on eMIPs (b) in buffer with the sandwich assay.

Equine PCT. As already performed for cPCT, the analysis of ePCT was carried out by replacing the capture antibody of the commercial ELISA kit with PNE-based eMIP and a sandwich test was developed by using a biotinylated secondary antibody (conjugated to an enzyme) as a last step before quantification (provided in the commercial kit). The analysis of the dilutions of ePCT used as the standard (50.0, 100, 200, 400 and 600 ng mL^{-1}) generated a calibration curve with a correlation coefficient of 0.987 (Fig. 3b). In detail, three different curves based on the analysis of triplicate standard solutions were considered to obtain the graph. The developed assay resulted in a LOD of 2.28 ng mL^{-1} and a LOQ of 7.61 ng mL^{-1}, with a CV_{av}% intra-assay and inter-assay of 4.16% and 4.78% respectively.

Plasma sample analysis

MIP selectivity. Regarding the selectivity of the imprinted material, to express the ratio between the ability of the MIP in discriminating between the imprinted template and one or more other (similar or not) molecules, possibly present in the

Open Access Article. Published on 29 november 2022. Downloaded on 19-9-2025 23:44:33.
This article is licensed under a Creative Commons Attribution-NonCommercial 3.0 Unported Licence.

real sample under analysis, we refer here to a factor called the selectivity factor (α).[77] In particular, we have tested the blank plasma, containing all the possible competing molecules except for PCT (pooled plasma from healthy animals). Basically, our selectivity estimation is performed considering the assay responses when using plasma alone, in the absence (plasma − PCT) and in the presence (plasma + PCT) of the analyte. These responses appear significantly different, and this consideration is valid for all the tested 'plasma + PCT' concentrations. In detail, by considering α values ($\alpha = Q_{\text{MIP target}}/Q_{\text{MIP competitor}}$), where Q is the mean absorbance response of the lowest 'plasma + PCT' analyte concentration, we obtain α(ePCT) = 14.8 and α(cPCT) = 2.7. In both the cases, and in line with the accepted guidelines for the interpretation of α values, both confirm the consistency of our results in real matrices. This represents really the most complex situation that one could face, and undoubtedly represents the 'alpha factor', expressed as MIP (plasma + PCT)/MIP (plasma − PCT).

Canine PCT. To evaluate the performance of the novel MIP-based assay in a real matrix, pooled blank plasma samples were spiked with the respective protein and analyzed. This, at the moment, represents the most realistic simulation due to several limitations. First, to classify plasma samples as "septic patients positive to PCT", a validated reference method for PCT quantification should be available. But this is actually the main lack for this kind of diagnostics. Second, due to the lack of robust and validated methods for PCT detection in equine and canine species, the related reference ranges and cut-off values required to classify patients as positive/negative septic, on the basis of this biomarker, are not available. Therefore, classifying animals as healthy or sick under these conditions is potentially highly misleading and risky, eventually penalizing our method.

Accordingly, different dilutions of the plasma samples, fortified with cPCT, were compared in order to obtain the maximum output signal and to reduce the residual nonspecific response in plasma. In detail, cPCT was spiked in pooled blank plasma at 25.0, 50.0 and 100 ng mL^{-1} and 1 : 2, 1 : 5, and 1 : 10 diluted with dilution buffer provided in the kit. Moreover, "as it is" plasma samples fortified with cPCT at the same concentrations were tested. The results reported in Fig. 4 show that the undiluted plasma gave a negligible signal, due to some plasma component that impaired the test function, while the 1 : 10 dilution allowed the best signal. This is likely related to the dilution of some plasma components that tend to unspecifically adsorb to the MIP, reducing the availability of specific recognition sites for the target protein. As a result, after 1 : 10 dilution, the signal significantly increased the dilution of the matrix.

The 1 : 10 dilution was the most favourable condition for the detection of cPCT in plasma samples. This dilution was thus selected for cPCT quantification. For this aim, cPCT was spiked in diluted plasma (1 : 10 with buffer) for a final concentration of

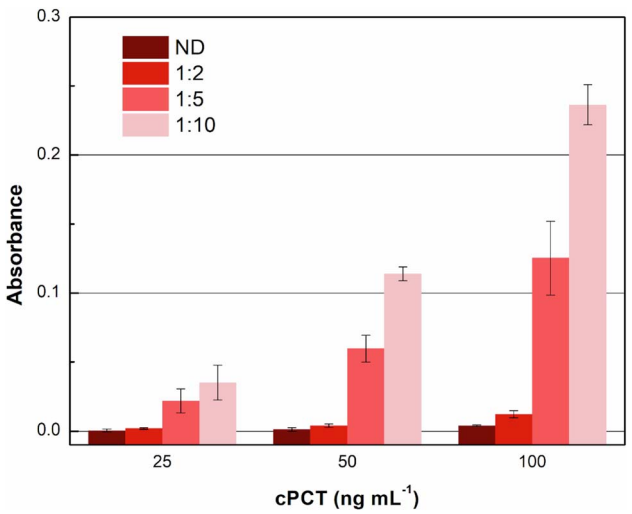

Fig. 4 Procalcitonin (PCT) sandwich assays in canine plasma samples diluted and fortified with cPCT (25.0, 50.0, 100 ng mL^{-1}). Samples were tested undiluted (ND) and at different dilutions (1 : 2, 1 : 5 and 1 : 10, respectively). Three replicates for each concentration.

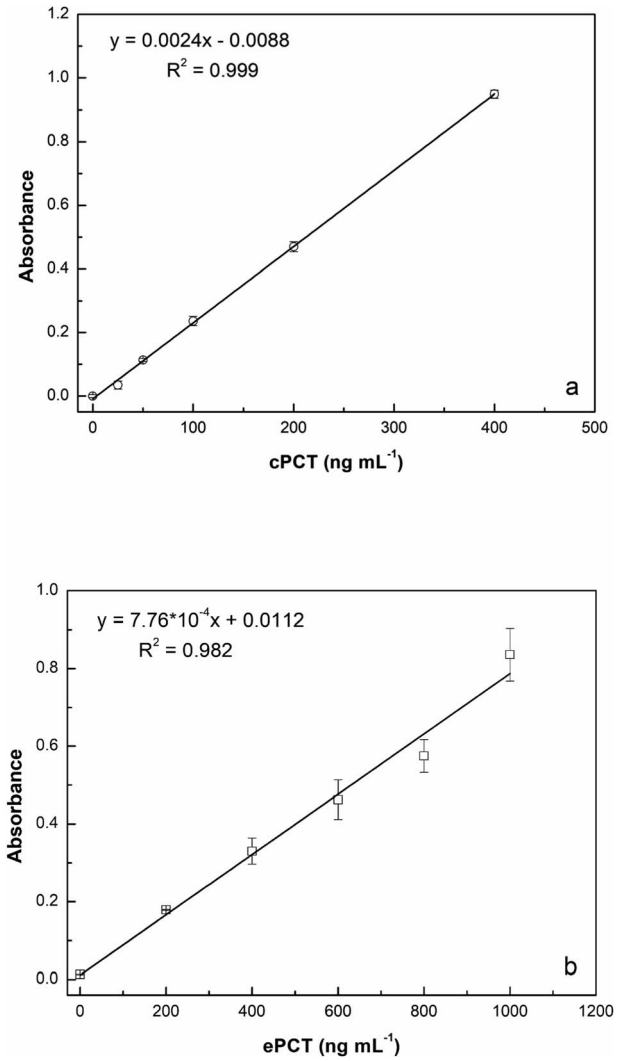

Fig. 5 Linear fitting obtained for cPCT on cMIPs and ePCT on eMIPs in species-specific plasma (diluted 1 : 10) with the sandwich assay (nonspecific signals were subtracted).

This journal is © The Royal Society of Chemistry 2023

Open Access Article. Published on 29 november 2022. Downloaded on 19-9-2025 23:44:33.
This article is licensed under a Creative Commons Attribution-NonCommercial 3.0 Unported Licence.

25.0, 50.0, 100, 200 and 400 ng mL^{-1} for testing. As reported in Fig. 5a, the assay displays a linear response with cPCT concentrations, showing an excellent linear correlation (R^2 = 0.999). The calibration range of cPCT in plasma resulted in 25–400 ng mL^{-1}, showing a lower slope than in the buffer. The resulting LOD and LOQ were, respectively, 5.87 and 19.6 ng mL^{-1}, with a CV_{av}% of 10.0% *vs.* 6.57% obtained in buffer, but still in line with the EMA guidelines.[78]

Equine PCT. The commercial ELISA kits that are generally reported in the literature for ePCT detection are not fully validated. An exception is a study by Rieger and collaborators, in which they developed an ELISA sandwich, for ePCT detection, based on human anti-PCT antibodies, thanks to the homology between equine and human proteins (83%).[73,79] In fact, to our current knowledge anti-equine antibodies are not commercially available. Moreover, a recent study showed that one of the commercially available ELISA kits for the measurement of ePCT did not detect the recombinant standard protein, whereas the human PCT ELISA kit was found suitable to detect the equine biomarker.[62] On this basis, the detection of ePCT in plasma samples was also performed with an ELISA kit for human PCT (DuoSet® ELISA). As for cPCT, different dilutions of plasma fortified with ePCT were compared (1 : 2, 1 : 5 and 1 : 10). Once again, the 1 : 10 dilution has been demonstrated to improve the output signal (data not shown). Analysis of dilutions of the recombinant equine protein in 1 : 10 diluted plasma (200, 400, 600, 800 and 1000 ng mL^{-1}) generated a calibration curve with a R^2 of 0.982 (Fig. 5b). The observed trend in plasma is very similar to that obtained in buffer; in contrast, the slope is significantly lower in the matrix than in the buffer and thus worse LOD and LOQ were estimated respectively at 4.46 ng mL^{-1} and 14.9 ng mL^{-1}. On the other hand, the reproducibility, expressed as an average of coefficient of variation, was confirmed to be optimal also in plasma samples with values of 5.43% (intra-assay) and 7.61% (inter-assay).

In this study, for the first time, a PNE-based mimetic receptor was produced onto disposable 96-well microplates for detection of ePCT and cPCT. To the best of our knowledge, for PCT detection in animal species, there are only sandwich ELISA tests, completely based on antibodies, available on the market and not applicable in the clinical field. None of the well-conceived studies in the literature succeeded in the development of innovative analytical methods for the determination of these biomarkers in veterinary medicine. Moreover, in the context of biomimetic receptors, the only example available in the literature reports an optical biosensor based on a molecularly imprinted polymer for the real-time detection of human procalcitonin.[80] Therefore, in this work, we aimed to realize new MIP-based sandwich assays for equine and canine PCT detection, in which biomimetic receptors were employed as target-capturing probes. The assay was capable of measuring e/c PCT in buffer and in untreated plasma (except for 1 : 10 dilution), thus being particularly useful in terms of speed and simplicity. The sensitivity of the assay, for ePCT quantification, is in accordance with the clinical performance demonstrated by previous studies in which home-made ELISA assay, based on human anti-PCT antibody, were used. Furthermore, Battaglia *et al.* (2020) have validated a commercially available ELISA assay based on human anti-PCT antibodies, by using an external standard, but showing a LOD of 56.0 ng mL^{-1} in plasma, significantly higher than the ePCT pseudo-ELISA assay here reported (4.46 ng mL^{-1}). Anyway, it is difficult to establish an optimal LOD value for PCT detection assay in veterinary medicine since little information is still available on the reference ranges as well as cut-off values for the lack of validated analytical methods.

Conclusions

A sandwich pseudo-ELISA method that exploits molecularly imprinted nanofilms as artificial antibodies for the detection of equine and canine PCT is presented. This method exhibited good performance both in buffer and plasma, suggesting a possible application to detect PCT in real dog and horse samples. The binding capacity, as well as the synthesis conditions of MIPs for both biomarkers were previously tested *via* a SPR platform by developing the polymer on the surface of gold chips. Here, the innovative assay has been developed allowing detection of the targets by using a portable, low-cost, and common platform, the ELISA microplate reader. Based on commercially available kits in the novel assay, working in a sandwich format, the capture antibody was replaced with a PNE-based MIP and secondary biotinylated Ab was maintained to bind S-HRP and to give a colorimetric signal. This ELISA method was able to detect both the biomarkers (canine and equine PCT) in buffer and in plasma samples (diluted 1 : 10). Under optimal conditions, the results obtained in plasma samples showed a limit of detection and a reproducibility of 5.87 ng mL^{-1} and 10.0% respectively for the canine sample and 4.46 ng mL^{-1} and 7.61% for the equine sample. Future studies could be dedicated to further improve the detection limit, by using more sensitive detection strategies such as fluorescence, and to accelerate the transition to a completely antibody-free assay. In this context, catecholamine-based MIPs, norepinephrine in this case, have shown to be a performing and very promising material for new generation MIPs, suitable for the effective detection of peptides and proteins in disposable microplates. The aim here was to maintain the routine protocol of commercial "ready to use" ELISA assay while introducing new and attractive elements as MIPs, in order to enhance the final assay in terms of stability, cost-effectiveness and reusability and open up new possibilities in the scenario of point of care (POC) tests. Moreover, to get closer to the real applicability of the method, in the future, the purpose of an advanced stage of this work could be the collection, over time, of "suspected septic patients" to be tested and the subsequent correlation analysis between the experimental results obtained by this method and the other traditional clinical evidence of sepsis.

Ethics declarations

An owner's written consent was obtained for the collection of plasma for the horses and dogs included in this study.

Open Access Article. Published on 29 november 2022. Downloaded on 19-9-2025 23:44:33.
This article is licensed under a Creative Commons Attribution-NonCommercial 3.0 Unported Licence.

Author contributions

Federica Battaglia: conceptualization, methodology, investigation, writing—original draft preparation, writing—review & editing. Francesca Bonelli: visualization, project administration, funding acquisition. Micaela Sgorbini: visualization, project administration, funding acquisition. Luigi Intorre: writing—review & editing, supervision, project administration, funding acquisition. Maria Minunni: writing—review & editing, supervision. Simona Scarano: conceptualization, methodology, investigation, data curation, review & editing, supervision. Valentina Meucci: conceptualization, methodology, investigation, data curation, writing—review & editing, supervision, project administration, funding acquisition.

Conflicts of interest

There are no conflicts to declare.

Acknowledgements

This research did not receive any specific grant from funding agencies, commercial, or not-for-profit sectors.

Notes and references

1 X. Fu, Y. Liu, R. Qiu, M. F. Foda, Y. Zhang, T. Wang and J. Li, *Biochem. Biophys. Rep.*, 2018, **13**, 73–77.
2 S. Wang, Y. Liu, S. Jiao, Y. Zhao, Y. Guo, M. Wang and G. Zhu, *J. Agric. Food Chem.*, 2017, **65**(46), 10107–10114.
3 K. Xu, H. Long, R. Xing, Y. Yin, S. A. Eremin, M. Meng and R. Xi, *Talanta*, 2017, **164**, 341–347.
4 Z. Liu, B. Zhang, J. Sun, Y. Yi, M. Li, D. Du, F. Zhu and J. Luan, *Sci. Total Environ.*, 2018, **613–614**, 861–865.
5 A. Padoan, F. Bonfante, M. Pagliari, A. Bortolami, D. Negrini, S. Zuin, D. Bozzato, C. Cosma, L. Sciacovelli and M. Plebani, *EBioMedicine*, 2020, **62**, 103101.
6 T. Peng, Y. Zong, M. Di Johnson, S. V. Menghani, M. L. Lewis and J. N. Galgiani, *Diagn. Microbiol. Infect. Dis.*, 2021, **99**(1), 115198.
7 R. M. Lequin, *Clin. Chem.*, 2005, **51**(12), 2415–2418.
8 G. N. Konstantinou, *Methods Mol. Biol.*, 2017, **1592**, 79–94.
9 G. Gonzalez-Sapienza, M. A. Rossotti and S. Tabares-da Rosa, *Front. Immunol.*, 2017, **8**, 997.
10 A. Zhang, W. Long, Z. Guo, G. Liu, Z. Hu, Y. Huang, Y. Li, T. M. Grabinski, J. Yang, P. X. Zhao, A. D. Everett, Y. Zhang and B. B. Cao, *J. Immunol. Methods*, 2010, **355**(1–2), 61–67.
11 P. Rebelo, E. Cosa-Rama, I. Seguro, J. G. Pacheco, H. P. A. Nouws, M. N. D. S. Cordeiro and C. Delerue-Matos, *Biosens. Bioelectron.*, 2021, **172**, 112719.
12 F. Cui, Z. Zhou and H. S. Zhou, *Sensors*, 2020, **20**(4), 996.
13 J. Liu, Y. Wang, X. Liu, Q. Yuan, Y. Zhang and Y. Li, *Talanta*, 2019, **199**, 573e580.
14 P. Palladino, M. Minunni and S. Scarano, *Biosens. Bioelectron.*, 2018, **106**, 93–98.
15 A. Turco, S. Corvaglia, E. Mazzotta, P. Pompa and C. Malitesta, *Sens. Actuators, B*, 2018, **255**, 3374–3383.
16 W. Zhao, H. Yang, S. Xu, J. Cai, J. Luo, W. Wei, X. Liu and Y. Zhu, *Colloids Surf., A*, 2018, **555**, 95e102.
17 T. Vaneckova, J. Bezdekova, G. Han, V. Adam and M. Vaculovicova, *Acta Biomater.*, 2020, **101**, 444–458.
18 K. Haupt, P. X. Medina Rangel and B. Tse Sum Bui, *Chem. Rev.*, 2020, **120**, 9554–9582.
19 J. J. BelBruno, *Chem. Rev.*, 2019, **119**, 94–119.
20 M. J. Whitcombe, I. Chianella, L. Larcombe, S. A. Piletsky, J. Noble, R. Porter and A. Horgan, *Chem. Soc. Rev.*, 2011, **40**, 1547–1571.
21 R. Thoelen, R. Vansweevelt, J. Duchateau, F. Horemans, J. D'Haen, L. Lutsen, D. Vanderzande, M. Ameloot, M. vandeVen, T. J. Cleij and P. Wagner, *Biosens. Bioelectron.*, 2008, **23**(6), 913–918.
22 L. Fang, M. Jia, H. Zhao, L. Kang, L. Shi, L. Zhou and W. Kong, *Trends Food Sci. Technol.*, 2021, **116**, 387–404.
23 Y. Bow, E. Sutriyono, S. Nasir and I. Iskandar, *Int. J. Adv. Sci. Eng. Inf. Technol.*, 2017, **7**(2), 662–668.
24 A. E. Radi, T. Wahdan and A. El-Basiony, Electrochemical Sensors Based on Molecularly Imprinted Polymers for Pharmaceuticals Analysis, *Curr. Anal. Chem.*, 2019, **14**(3), 219–239.
25 B. Hatamluyi, A. Hashemzadeh and M. Darroudi, *Sens. Actuators, B*, 2020, **307**, 127614.
26 M. R. Ali, M. S. Bacchu, M. R. Al-Mamun, M. M. Rahman, M. S. Ahommed, M. A. Saad Aly and M. Z. H. Khan, *J. Mater. Sci.*, 2021, **56**, 12803–12813.
27 Z. Mazouz, M. Mokni, N. Fourati, C. Zerrouki, F. Barbault, M. Seydou, R. Kalfat, N. Yaakoubi, A. Omezzine, A. Bouslema and A. Othmane, *Biosens. Bioelectron.*, 2020, **151**, 111978.
28 M. Pirzada, E. Sehit and Z. Altintas, *Biosens. Bioelectron.*, 2020, **166**, 112464.
29 Z. X. Xu, H. J. Gao, L. M. Zhang, X. Q. Chen and X. G. Qiao, *Food Sci.*, 2011, **76**(2), 69–75.
30 C. Chen, J. Luo, C. Li, M. Ma, W. Yu, J. Shen and Z. Wang, *J. Agric. Food Chem.*, 2018, **66**, 2561–2571.
31 C. Zhang, H. Cui, Y. Han, F. Yu and X. Shi, *Anal. Methods*, 2018, **240**, 893–897.
32 L. Li, Z. Z. Lin, A. H. Peng, H. P. Zhong, X. M. Chen and Z. Y. Huang, *J. Chromatogr., Biomed. Appl.*, 2016, **1035**, 25–30.
33 C. Guoning, G. Pengqi, W. Yan, W. Lu, S. Hua, L. Yunzhe, J. Wanghui, C. Chun and F. Qiang, *Talanta*, 2019, **198**, 55–62.
34 S. P. Tang, F. Canfarotta, K. Smolinska-Kempisty, E. Piletska, A. Guerreiro and S. Piletsky, *Anal. Methods*, 2017, **9**, 2853–2858.
35 F. Torrini, L. Caponi, A. Bertolini, P. Palladino, F. Cipolli, A. Saba, A. Paolicchi, S. Scarano and M. Minunni, *Anal. Bioanal. Chem.*, 2022, **414**, 5423–5434.
36 J. Liu, Q. Deng, D. Tao, K. Yang, L. Zahng, Z. Liang and Y. Zhang, *Sci. Rep.*, 2014, **4**, 5487.
37 P. Palladino, F. Bettazzi and S. Scarano, *Anal. Bioanal. Chem.*, 2019, **411**, 4327–4338.
38 C. Xie, X. Wang, H. He, Y. Ding and X. Lu, *Adv. Funct. Mater.*, 2020, **30**(25), 1909954.
39 J. H. Ryu, P. B. Messersmith and H. Lee, *ACS Appl. Mater. Interfaces*, 2018, **10**(9), 7523–7540.

 This journal is © The Royal Society of Chemistry 2023

Open Access Article. Published on 29 november 2022. Downloaded on 19-9-2025 23:44:33.
This article is licensed under a Creative Commons Attribution-NonCommercial 3.0 Unported Licence.

40 V. Baldoneschi, P. Palladino, S. Scarano and M. Minunni, *Anal. Bioanal. Chem.*, 2020, **412**(24), 5945–5954.
41 A. Lamaoui, J. M. Palacios-Santander, A. Amine and L. Cubillana-Aguilera, *Microchem. J.*, 2021, **164**, 106043.
42 G. H. Yao, R. P. Liang, C. F. Huang, Y. Wang and J. D. Qiu, *Anal. Chem.*, 2013, **85**(24), 11944–11951.
43 J. Miao, A. Liu, L. Wu, M. Yu, W. Wei and S. Liu, *Anal. Chim. Acta*, 2020, **1095**, 82–92.
44 J. Yin, Z. Meng, M. Du, C. Liu, M. Song and H. Wang, *J. Chromatogr. A*, 2010, **1217**, 5420e5426.
45 A. Tretjakov, V. Syritski, J. Reut, R. Boroznjak, O. Volobujeva and A. Opik, *Microchim. Acta*, 2013, **180**, 1433–1442.
46 B. Yang, S. Lv, F. Chen, C. Liu, C. Cai, C. Chen and X. Chen, *Anal. Chim. Acta*, 2016, **912**, 125–132.
47 Y. Sun and S. Zhong, *Colloids Surf., B*, 2017, **159**, 131–138.
48 X. Xu, R. Liu, P. Guo, Z. Luo, X. Cai, H. Shu, Y. Ge, C. Chang and Q. Fu, *Food Chem.*, 2018, **256**, 91–97.
49 W. Chen, M. Fu, X. Zhu and Q. Liu, *Biosens. Bioelectron.*, 2019, **142**, 111492.
50 X. Liu, W. Lin, P. Xiao, M. Yang, L.-P. Sun, Y. Zhang, W. Xue and B.-O. Guan, *Chem. Eng. J.*, 2020, **387**, 124074.
51 A. H. Nadim, M. A. Abd El-Aal, M. A. Al-Ghobashy and Y. S. El-Saharty, *Microchem. J.*, 2021, **167**, 106333.
52 S. Hong, J. Kim, Y. S. Na, J. Park, S. Kim, K. Singha, G. Im, D. K. Han, W. J. Kim and H. Lee, *Angew. Chem.*, 2013, **52**(35), 9187–9191.
53 V. Baldoneschi, P. Palladino, M. Banchini, M. Minunni and S. Scarano, *Biosens. Bioelectron.*, 2020, **157**, 112161.
54 F. Battaglia, V. Baldoneschi, V. Meucci, L. Intorre, M. Minunni and S. Scarano, *Talanta*, 2021, **230**, 122347.
55 M. Jin and A. I. Khan, *Lab. Med.*, 2010, **41**(3), 173–177.
56 J. Davies, *J. Clin. Pathol.*, 2015, **68**(9), 675–679.
57 M. Meisner, *Procalcitonin: Biochemistry and Clinical Diagnosis*, UNI-MED, Verlag AG, 1st edn, 2010.
58 A. L. Vijayan, S. Ravindran, R. Saikant, S. Lakshmi, R. Kartik and G. Manoj, *J. Intensive Care*, 2017, **5**, 51.
59 E. Matur, E. Eraslan and Ü. Çötelioğlu, *J. Istanbul Vet. Sci.*, 2017, **2**(1), 16–27.
60 M. J. López-Martínez, L. Franco-Martínez, S. Martínez-Subiela and J. J. Cerón, *Anim. Health Res. Rev.*, 2021, **23**, 82–99.
61 I. Nocera, F. Bonelli, V. Vitale, V. Meucci, G. Conte, E. Jose-Cunilleras, L. A. Gracia-Calvo and M. Sgorbini, *Animals*, 2021, **11**, 2015.
62 W. El-Deeb, M. Fayez, I. Elsohaby, H. V. Mkrtchyan and A. Alhaider, *Comp. Immunol., Microbiol. Infect. Dis.*, 2020, **73**, 101525.
63 F. Bonelli, V. Meucci, T. J. Divers, E. Jose-Cunilleras, M. Corazza, R. Tognetti, G. Guidi, L. Intorre and M. Sgorbini, *J. Vet. Intern. Med.*, 2015, **29**, 1689–1691.
64 I. Kilcoyne, J. E. Nieto and J. E. Dechant, *J. Am. Vet. Med. Assoc.*, 2020, **256**, 927–933.
65 M. C. Costa, G. Silva, R. V. Ramos, H. R. Staempfli, L. G. Arroyo, P. Kim and J. S. Weese, *Vet. J.*, 2016, **205**, 74–80.
66 Z. Yilmaz, Y. O. Ilcol and I. H. Ulus, *Crit. Care Med.*, 2008, **85**(24), 11944–11951.
67 R. Troia, M. Giunti and R. Goggs, *BMC Vet. Res.*, 2018, **14**, 111.
68 R. Goggs, M. Milloway, R. Troia and M. Giunti, *Vet. Rec. Open*, 2018, **5**, e000255.
69 F. Easley, M. K. Holowaychuk, E. W. Lashnits, S. K. Nordone, H. Marr and A. J. Birkenheuer, *J. Vet. Intern. Med.*, 2020, **34**(2), 653–658.
70 F. Bonelli, V. Meucci, T. J. Divers, A. Boccardo, D. Pravettoni, M. Meylan, A. G. Belloli and M. Sgorbini, *Vet. J.*, 2018, **234**, 61–65.
71 N. Ercan, N. Tuzcu, O. Başbug, M. Tuzcu and A. Alim, *J. Vet. Diagn. Invest.*, 2016, **28**, 180–183.
72 F. Battaglia, V. Meucci, R. Tognetti, F. Bonelli, M. Sgorbini, G. Lubas, C. Pretti and L. Intorre, *Animals*, 2020, **10**(9), 1511.
73 M. Rieger, C. Kochleus, D. Teschner, D. Rascher, A. K. Barton, A. Geerlof, E. Kremmer, M. Schmid, A. Hartmann and H. Gehlen, *Anal. Bioanal. Chem.*, 2014, **406**(22), 5507–5512.
74 D. Teschner, M. Rieger, C. Koopmann and H. Gehlen, *PFERDEHEILKUNDE*, 2015, **31**(4), 371–377.
75 A. K. Barton, A. Pelli, M. Rieger and H. Gehlen, *BMC Vet. Res.*, 2016, **12**, 5–7.
76 A. N. K. Floras, M. K. Holowaychuk, D. C. Hodgins, H. S. Marr, A. Birkenheuer, S. Sharif, A. M. E. Bersenas and D. Bienzle, *J. Vet. Intern. Med.*, 2014, **28**(2), 599–602.
77 A. M. Mostafa, S. J. Barton, S. P. Wren and J. Barker, *Trends Anal. Chem.*, 2021, **144**, 116431.
78 EMA, *Guideline on Bioanalytical Method Validation*, 2011, **https://www.ema.europa.eu/en/documents/scientific-guideline/guideline-bioanalytical-method-validation_en.pdf**, accessed 15 April 2022.
79 R. E. Toribio, C. W. Kohn, G. W. Leone, C. C. Capen and T. J. Rosol, *Mol. Cell. Endocrinol.*, 2003, **199**(1–2), 119–128.
80 G. Sener, E. Ozgur, A. Y. Rad, L. Uzun, R. Say and A. Denizli, *Analyst*, 2013, **138**(21), 6422–6428.